Available at
http://pvamu.edu/aam
Appl. Appl. Math.
ISSN: 1932-9466

Applications and Applied Mathematics:
An International Journal
(AAM)

Special Issue No. 4 (March 2019), pp. 82 – 96

Radiation effect on mixed convection flow of nanofluid between two concentric cylinders with Hall and Ion-slip effects

[1]Md. Shafeeurrahman and [2]D. Srinivasacharya

Department of Mathematics
Vaagdevi College of Engineering
Warangal-506005, India
[1]rahaman16@gmail.com; [2]dsrinivasacharya@gmail.com

Received: August 8, 2018; Accepted: October 28, 2018

Abstract

This paper analyzes the effects of thermal radiation, Hall and ion slip parameter on mixed convective nanofluid flow in an annuli between two concentric cylinders in the existence of strong magnetic field. The nonlinear governing equations are non-dimensionalized and then solved by using homotopy analysis method. The influence of radiation, magnetic, Hall and ion slip parameters on the velocity, temperature, nanoparticle concentration, Nusselt number and nanoparticle Sherwood number are investigated and represented graphically.

Keywords: Nanofluid; Radiation; Mixed convection; Concentric cylinders; Hall effect; Ion slip effect; Homotopy analysis method

MSC 2010 No.: 76R10, 76D05, 74F05, 76S05, 14F35

1. Introduction

Heat transfer and mixed convection flow of nanofluid in annulus between two concentric cylinders is an important phenomena in the system of Engineering in view of its enormous range of applications in thermal storage systems, thermal insulation, solar energy systems, compact heat exchangers, nuclear reactors, aircraft fuselage insulation to underground electrical transmission cables, boilers, cooling of electronic devices, cooling core of nuclear reactors, cooling systems, gas-cooled electrical cables and electrical gas insulated transmission lines. A number of researchers have studies convective heat transfer flows in annulus region between two concentric cylinders (See Dawood (2015) for review of such flows).

Nanofluids, first pioneered by Choi (1995), consists of uniformly suspended and dispersed nanometer sized particles in a base fluid. As these fluids have a higher thermal conductivity than the base fluids, they are used for developing both thermal conductivity and suspension stability in the different industrial systems. Several investigators have analyzed the mixed convection flow and heat transfer of nanofluids in an annular passages under various aspects.

The influence of thermal radiation on nanofluid can be most important in applications of space technology and at high operating temperature. In many areas of thermal radiation effect on combination of free and forced convection flow have not been studies since thermal radiation is a complicated parameter. Therefore the researchers have a great opportunity and significance to investigate on radiative flow of nanofluid. Srinivasacharya and Shafeeurrahman (2017) studied the effects of radiation and Joule heating on mixed convective nanofluid between two concentric cylinders. The effects of radiation and rotation on MHD chemically reacting nanofluid flow past a permeable flat plate with in porous medium examined by Ramanareddy et al. (2016).

Convective heat exchange and fluid flow problems with the interaction of magnetic field have attracted much attention due to the several astrophysics and industrial applications. The applications include study of solar plasma, stellar structures, and terrestrial cores. In industrial processes the extraction of geothermal energy, nuclear reactors, metallurgical and crystal growth in the field of semiconductors. Chamkha et al. (2015) presented a review on various research work done on MHD convection of nanofluids in various geometries and applications. Mozayyeni and Rahimi (2012) studied the mixed convective flow in cylindrical annulus with an effect in the radial direction and constant magnetic field with rotating outer cylinder. Ashorynejad et al. (2013) investigated numerically the mixed convective heat transfer in an annuli of horizontal cylinder filled with nanofluid considering the significance of constant radial magnetic field on the fluid. Sheikholeslami et al. (2015, 2017, 2017) studied the influence of magnetic field on nanofluid flow, heat and mass transfer in between two horizontal coaxial cylinders using a two-phase model. Das et al. (2015) analyses the mixed convective nanofluid flow in a concentric cylindrical pipes considering a uniform magnetic field.

In the investigations concerned with the MHD convective flows, Hall current and ion slip terms in Ohms law were neglected in order to simplify the mathematical analysis of the problem. However, the significance of Hall current and ion slip are essential in the presence of strong magnetic field. Therefore, in several physical situations it is required to include the effect of Hall current and ion slip terms in the MHD equations. The effects of Hall term on electrically conducting steady viscous fluid in channels was studied by Tani (1962). Satya Narayana et al.(2013) studied the effects of Hall current and radiation absorption on MHD micropolar fluid in a rotating system. Rajput et al. (2017, 2018) examined the rotation and radiation effects on MHD flow past an inclined plate with variable wall temperature and mass diffusion in the presence of Hall current. Hayat et al. (2016) addressed the mixed convective peristaltic flow of nanofluid in a channel with Hall and ion slip effects. Hall and ion slip effects on mixed convection flow of nanofluid between two concentric cylinders is analyzed by Srinivasacharya and Shafeeurrahman (2017). Hazarika (2014) has analyzed Hall current in a rotating channel on MHD flow with radiation and viscous dissipation.

The preceding literature reveals that the problem of heat transfer in mixed convective nanofluid

flow in a concentric cylinders with effects of radiation, Hall current and ion slip parameter has not only considered, but also the interaction of Hall current, ion slip effects with magnetic nano particles in a mixed convection flow presents an interesting fluid dynamics problem. Hence, the aim of the present paper is to find the influence of radiation, Hall current and ion slip parameter on the flow of mixed convection and heat transfer nanofluid in concentric cylinders. The HAM procedure is used to find the solution of the nonlinear differential equations. The HAM method was first introduced by Liao (2003), which is one of the most powerful techniques to solve various types of strongly nonlinear equations. The effect of flow parameters on the profiles of dimensionless velocity, temperature and nanoparticle concentration is examined.

2. Formulation of the problem

Consider steady, laminar and incompressible nanofluid flow in an annular space between two infinitely long concentric cylinders of radius a and b $(a < b)$ and kept at temperatures T_a and T_b, respectively. Choose cylindrical polar coordinates system (r, ψ, z) with $z-$ axis along the common axis of cylinders and r normal to the $z-$axis. Assume that the outer cylinder is rotating with constant angular velocity Ω whereas the inner cylinder is at rest. The flow is induced due to the rotation of the exterior cylinder. A strong magnetic field B_0 is taken in an axial direction. Comparison with the applied magnetic field, the induced magnetic field can be ignored with the assumption of magnetic Reynolds number is very low. Assume relatively high electron-atom collision frequency so that the impact of Hall, ion slip cannot be omitted. Thermophysical characteristics of the nanofluid are taken as constant except density in the buoyancy term of the balance of momentum equation. In addition, the Brownian motion and thermophoresis effects are incorporated (2006). The velocity component along ψ direction, temperature, concentration and nanoparticle volume fraction are denoted by is u, T and ϕ, respectively.

The equations which govern the present flow (2006) with Boussinesq approximation are

$$\frac{\partial u}{\partial \psi} = 0, \tag{1}$$

$$\frac{\partial p}{\partial r} = \frac{\rho u^2}{r} - \frac{\sigma\, B_0^2\, \beta_h\, u}{(\alpha_e^2 + \beta_h^2)}, \tag{2}$$

$$\begin{aligned} \mu \frac{\partial}{\partial r}\left[\frac{1}{r}\frac{\partial}{\partial r}(r\,u)\right] + (1-\phi)\rho_f g\left[\beta_T (T - T_a)\right] - (\rho_p - \rho_f)\, g(\phi - \phi_a) \\ - \frac{\sigma\, B_0^2\, \alpha_e\, u}{(\alpha_e^2 + \beta_h^2)} - \frac{1}{r}\frac{\partial p}{\partial \psi} = 0, \end{aligned} \tag{3}$$

$$\begin{aligned} \alpha\left[\frac{\partial^2 T}{\partial r^2} + \frac{1}{r}\frac{\partial T}{\partial r}\right] + \frac{\mu}{\rho c_p}\left[\left(\frac{\partial u}{\partial r}\right)^2 - 2\,\frac{u}{r}\frac{\partial u}{\partial r} + \left(\frac{u}{r}\right)^2\right] \\ - \frac{1}{\rho c_p}\nabla . q_r + \tau\left[D_B \frac{\partial T}{\partial r}\frac{\partial \phi}{\partial r} + \frac{D_T}{T_0}\left(\frac{\partial T}{\partial r}\right)^2\right] = 0, \end{aligned} \tag{4}$$

$$D_B\left[\frac{\partial^2 \phi}{\partial r^2} + \frac{1}{r}\frac{\partial \phi}{\partial r}\right] + \frac{D_T}{T_0}\left[\frac{\partial^2 T}{\partial r^2} + \frac{1}{r}\frac{\partial T}{\partial r}\right] = 0, \tag{5}$$

where the electrical conductivity is σ, density is ρ, pressure is p, specific heat capacity is C_p, thermal diffusion ratio is K_T, viscosity coefficient is μ, acceleration due to gravity is g, ion slip parameter is βi, Hall parameter is β_h, Brownian diffusion coefficient is D_B, $\alpha_e = 1 + \beta_h\,\beta i$ is a constant, mean fluid temperature is T_0, coefficients of thermal expansion is β_T, effective thermal diffusivity is α, thermophoretic diffusion coefficient is D_T, coefficient of thermal conductivity is $k_f = \alpha\,(\rho\,C)_p$, the ratio of heat capacity of the fluid and effective heat capacity of the nanoparticle material is τ and the radiation heat flux is q_r, under the Rosseland approximation we assume q_r as

$$q_r = -\frac{4\sigma^*}{3\chi}\,\frac{\partial T^4}{\partial y}, \tag{6}$$

where Stefan-Boltzman constant is σ^*, coefficient of mean absorption is χ. We assume the variation in fluid phase temperature inside the flow to be appropriately minimum such that T^4 may be shown as a linearly continuous function of the temperatures and enlarged in a Taylor series around T_0 and removing highest order terms we get $T^4 = 4T_0^3\,T - 3T_0^4$.

The boundary conditions are

$$u = 0,\ \ T = T_a,\ \ \phi = \phi_a \ \text{ at } \ r = a, \tag{7a}$$

$$u = b\Omega,\ \ T = T_b,\ \ \phi = \phi_b \ \text{ at } \ r = b. \tag{7b}$$

Introducing the following non-dimensional variables

$$\lambda = \frac{r^2}{b^2},\ f(\lambda) = \frac{u\sqrt{\lambda}}{\Omega}, \theta = \frac{T - T_a}{T_b - T_a},\ S = \frac{\phi - \phi_a}{\phi_b - \phi_a},\ P = \frac{bp}{\mu\,\Omega}, \tag{8}$$

in Equations (1) - (5), we get the nonlinear differential equations as

$$4\,f''\lambda + \sqrt{\lambda}\frac{G_r}{Re}\,(\theta - N_r S) - \frac{Ha^2\,\alpha_e\,f}{{\alpha_e}^2 + {\beta_h}^2} - A = 0, \tag{9}$$

$$\begin{aligned}&\left(1 + \frac{4}{3}\,Rd\right)(\lambda^3\theta'' + \lambda^2\theta') + B_r\,\left[\lambda^2(f')^2 - 2\,\lambda\,f\,f' + (f)^2\right]\\ &+P_r\,D_f(\lambda^3\varphi'' + \lambda^2\varphi') + P_r\,N_b\,\lambda^3\,\theta'\,S' + P_r\,N_t\,\lambda^2\,(\theta')^2 = 0,\end{aligned} \tag{10}$$

$$\lambda\,S'' + S' + \frac{N_t}{N_b}(\lambda\,\theta'' + \theta') = 0, \tag{11}$$

where the prime indicate derivative corresponding to λ, the Prandtl number is $Pr = \dfrac{\mu\,C_P}{k_f}$, Grashof number is $Gr = \dfrac{(1-\phi)\,g\,\beta_T(T_b - T_a)b^3}{\nu^2}$, Reynold's number is $Re = \dfrac{\rho\Omega b}{\mu}$, constant pressure gradient is $A = \frac{\partial P}{\partial \varphi}$, Hartman number is $Ha^2 = \dfrac{\sigma {B_0}^2\,b^2}{\mu}$, Brinkman number is $Br = \dfrac{\mu\,\Omega^2}{k_f\,(T_b - T_a)}$, Brownian motion parameter is $N_b = \dfrac{\tau\,D_B(\phi_b - \phi_a)}{\nu}$, thermoporesis parameter is $N_t = \dfrac{\tau\,D_T(T_b - T_a)}{T_m\,\nu}$, buoyancy ratio is $N_r = \dfrac{(\rho_p - \rho_f)(\phi_b - \phi_a)}{\rho_f\beta_T(T_b - T_a)(1-\phi)}$, and Radiation parameter is $Rd = \dfrac{4\sigma^*}{\chi}\,\dfrac{T_0^3}{k_f}$.

The corresponding boundary conditions (7) are

$$\begin{aligned} S = 0,\ \theta = 0,\ f = 0 \ \text{ at } \lambda = \lambda_0, \\ S = 1,\ \theta = 1,\ f = b \ \text{ at } \quad \lambda = 1. \end{aligned} \tag{12}$$

The main aim of this study is to obtain the parameters of nanofluid flow, heat and mass transfer problems, like Nu and NSh (Nusselt number, nanoparticle sherwood number, respectively). These parameters characterize the wall heat and nanoparticle mass transfer rates, respectively. The heat and nanoparticle mass fluxes in the concentric cylinders can be achieved from

$$q_w = -k_f \nabla T + q_r, \quad q_s = -D_B \nabla \phi. \tag{13}$$

The Nusselt number $Nu = \frac{b\, q_w}{k_f\,(T_b - T_a)}$, and the nanoparticle sherwood number $NSh = \frac{b\, q_s}{D_B\,(T_b - T_a)}$ are given by

$$\begin{aligned} Nu &= -2\left(1 + \frac{4}{3}Rd\right)\sqrt{\lambda}\left(\frac{\partial \theta}{\partial \lambda}\right)_{\lambda=0}, \\ NSh &= -2\sqrt{\lambda}\left(\frac{\partial S}{\partial \lambda}\right)_{\lambda=0}. \end{aligned} \tag{14}$$

3. Homotopy solution

The first step in HAM solution, is choosing the initial value of $f(\lambda)$, $\theta(\lambda)$ and $S(\lambda)$ and auxiliary linear operators.(For more details on homotopy analysis method see the works of Liao (2003, 2004, 2010, 2013). Therefore, we choose the initial approximations as

$$f_0(\lambda) = \frac{b\,(\lambda - \lambda_0)}{1 - \lambda_0}, \quad \theta_0(\lambda) = \frac{\lambda - \lambda_0}{1 - \lambda_0} \qquad \text{and} \quad S_0(\lambda) = \frac{\lambda - \lambda_0}{1 - \lambda_0}, \tag{15}$$

and the auxiliary linear operators as

$$L_i = \frac{\partial^2}{\partial \lambda^2} \quad \text{for} \quad i = 1, 2, 3, \tag{16}$$

such that

$$L_1(c_1 + c_2\lambda) = 0,\ L_2(c_3 + c_4\lambda) = 0 \quad and \quad L_3(c_5 + c_6\lambda) = 0, \tag{17}$$

where $c_i, (i = 1, 2, \cdots, 6)$, are constants. The second step in HAM is to defining the zeroth order deformation, which is given by

$$(1 - p)L_1[f(\lambda; p) - f_0(\lambda)] = p h_1 N_1[f(\lambda; p)], \tag{18}$$

$$(1 - p)L_2[\theta(\lambda; p) - \theta_0(\lambda)] = p h_2 N_2[\theta(\lambda; p)], \tag{19}$$

$$(1 - p)L_3[S(\lambda; p) - S_0(\lambda)] = p h_3 N_3[S(\lambda; p)], \tag{20}$$

where

$$N_1[f(\lambda,p),\theta(\lambda,p),S(\lambda,p)] = 4\,f''\lambda + \sqrt{\lambda}\frac{G_r}{Re}\,(\theta - N_r S) - \frac{Ha^2\,\alpha_e\,f}{{\alpha_e}^2 + {\beta_h}^2} - A, \tag{21}$$

$$\begin{aligned} N_2[f(\lambda,p),\theta(\lambda,p),S(\lambda,p)] &= \left(1+\frac{4}{3}\,Rd\right)(\lambda^3\theta'' + \lambda^2\theta') + P_r\,N_b\,\lambda^3\,\theta'\,S' \\ &+P_r\,D_f(\lambda^3\varphi'' + \lambda^2\varphi') + B_r\,\left[\lambda^2(f')^2 - 2\,\lambda\,f\,f' + (f)^2\right] + P_r\,N_t\,\lambda^2\,(\theta')^2, \end{aligned} \tag{22}$$

$$N_3[f(\lambda,p),\theta(\lambda,p),S(\lambda,p)] = \lambda\,S'' + S' + \frac{N_t}{N_b}(\lambda\,\theta'' + \theta'), \tag{23}$$

where $p \in [0,1]$ is the embedded parameter and h_i, $(i = 1,2,3)$ are auxiliary parameters which are not vanish. The equivalent boundary conditions are

$$\begin{aligned} &f(0;p) = 0, \quad \theta(0;p) = 0, \qquad S(0;p) = 0, \\ &f(1;p) = b, \quad \theta(1;p) = 1, \qquad S(1;p) = 1. \end{aligned} \tag{24}$$

Next, the deformation equations of m^{th}-order are given by

$$L_1[f_m(\lambda) - \chi_m f_{m-1}(\lambda)] = h_1 R_m^f(\lambda), \tag{25}$$

$$L_2[\theta_m(\lambda) - \chi_m \theta_{m-1}(\lambda)] = h_2 R_m^\theta(\lambda), \tag{26}$$

$$L_3[S_m(\lambda) - \chi_m S_{m-1}(\lambda)] = h_3 R_m^S(\lambda), \tag{27}$$

where

$$\left.\begin{aligned} R_m^f(\lambda) &= 4\,f''\lambda + \sqrt{\lambda}\frac{G_r}{R_e}\,(\theta - N_r S) - \frac{Ha^2\,\alpha_e\,f}{{\alpha_e}^2 + {\beta_h}^2} - A, \\ R_m^\theta(\lambda) &= \left(1+\frac{4}{3}\,Rd\right)(\lambda^3\theta'' + \lambda^2\theta') + P_r\,D_f(\lambda^3\varphi'' + \lambda^2\varphi') \\ &+B_r\left[\lambda^2\sum_{n=0}^{m-1} f'_{m-1-n}f'_n - 2\lambda\sum_{n=0}^{m-1} f_{m-1-n}f'_n + \sum_{n=0}^{m-1} f_{m-1-n}f_n\right] \\ &+P_r N_b\lambda^3\sum_{n=0}^{m-1}\theta'_{m-1-n}S'_n + P_r N_t\,\lambda^2\sum_{n=0}^{m-1}\theta'_{m-1-n}\theta'_n], \\ R_m^S(\lambda) &= \lambda\,S'' + S' + \frac{N_t}{N_b}(\lambda\,\theta'' + \theta'), \end{aligned}\right\} \tag{28}$$

for integer m

$$\begin{aligned} \chi_m &= 0 \quad \text{for} \quad m \le 1, \\ &= 1 \quad \text{for} \quad m > 1. \end{aligned}$$

From $p = 0$ to $p = 1$, we can have

$$f(\lambda;0) = f_0, \quad f(\lambda;1) = f(\lambda), \tag{29}$$

$$\theta(\lambda;0)=\theta_0, \quad \theta(\lambda;1)=\theta(\lambda), \tag{30}$$

$$S(\lambda;0)=S_0, \quad S(\lambda;1)=S(\lambda). \tag{31}$$

Thus, as p varying from 0 to 1, f, θ and S varies continuously from f_0, θ_0 and S_0 to final value $f(\lambda)$, $\theta(\lambda)$ and $S(\lambda)$, respectively. In view of Taylor's series f, θ and S can be written as

$$\begin{aligned}
f(\lambda;p) &= f_0+\sum_{m=1}^{\infty} f_m(\lambda)p^m, \quad f_m(\lambda)=\frac{1}{m!}\frac{\partial^m}{\partial p^m}f(\lambda;p)\Big|_{p=0},\\
\theta(\lambda;p) &= \theta_0+\sum_{m=1}^{\infty} \theta_m(\lambda)p^m, \quad \theta_m(\lambda)=\frac{1}{m!}\frac{\partial^m}{\partial p^m}\theta(\lambda;p)\Big|_{p=0},\\
S(\lambda;p) &= S_0+\sum_{m=1}^{\infty} S_m(\lambda)p^m, \quad S_m(\lambda)=\frac{1}{m!}\frac{\partial^m}{\partial p^m}S(\lambda;p)\Big|_{p=0},
\end{aligned} \tag{32}$$

we have to choose the values of the auxiliary parameters for which the series (32) are converge at $p=1$, i.e.,

$$\begin{aligned}
f(\lambda) &= f_0+\sum_{m=1}^{\infty} f_m(\lambda), \quad \theta(\lambda)=\theta_0+\sum_{m=1}^{\infty}\theta_m(\lambda),\\
&\qquad\qquad S(\lambda)=S_0+\sum_{m=1}^{\infty} S_m(\lambda).
\end{aligned} \tag{33}$$

4. Convergence

In HAM, it is essential to see that the series solution converges. Also, the rate of convergence of approximation for the HAM solution mainly calculate on the values of h. To find the admissible space of the auxiliary parameters, h curves are drown for 16^{th}-order of approximation and shown in Figure1. It is visible from this figure that the permissible interval for h_1, h_2 and h_3 is $-0.6 < h_1 < -0.0$, $-1.0 < h_2 < -0.3$ and $-1.8 < h_3 < -0.4$, respectively.

The following average residual errors (see Liao (2010)) are computed to obtain the optimal value of auxiliary parameter

$$\begin{aligned}
E_{f,m} &= \frac{1}{2K}\sum_{i=-K}^{K}\left(N_1\left[\sum_{j=0}^{m} f_j(i\triangle t)\right]\right)^2,\\
E_{\theta,m} &= \frac{1}{2K}\sum_{i=-K}^{K}\left(N_2\left[\sum_{j=0}^{m} \theta_j(i\triangle t)\right]\right)^2,\\
E_{S,m} &= \frac{1}{2K}\sum_{i=-K}^{K}\left(N_4\left[\sum_{j=0}^{m} S_j(i\triangle t)\right]\right)^2,
\end{aligned} \tag{34}$$

Table 1. At different order of approximations the optimal values of h_1, h_2 and h_3

	Optimal of h_1		Optimal of h_2		Optimal of h_3	
$Order$	h_1	Min of E_m	h_2	Min of E_m	h_3	Min of E_m
12	-0.09	1.02×10^{-3}	-0.71	6.51×10^{-4}	-1.18	2.92×10^{-5}
14	-0.10	1.93×10^{-3}	-0.69	8.29×10^{-4}	-1.16	3.68×10^{-4}
16	-0.10	2.79×10^{-3}	-0.69	1.11×10^{-5}	-1.18	9.73×10^{-4}

Table 2. Convergence of HAM solutions for different order of approximations.

Order	f(0.625)	$\theta(0.625)$	S(0.625)
05	0.4376535201	0.6737468076	0.6581184839
10	0.4406095166	0.6916338076	0.6219805748
15	0.4413595133	0.7055058072	0.6127974698
20	0.4420191206	0.7061768072	0.6020224807
25	0.4420194520	0.7172401678	0.6020226948
30	0.4420194612	0.7172472210	0.6020226464
35	0.4420194612	0.7172472807	0.6020226464
40	0.4420194612	0.7172472807	0.6020226464
45	0.4420194612	0.7172472807	0.6020226464
50	0.4420194612	0.7172472807	0.6020226464
55	0.4420194612	0.7172472807	0.6020226464

where $\triangle t = 1/K$ and $K = 5$. At various levels of approximations (m), least average residual errors are represented in Table 1. From this, we see that the average residual errors are least at $h_1 = -0.43$, $h_2 = -0.69$ and $h_3 = -1.1$. Therefore, the optimality of convergence control parameters are appropriated as $h_1 = -0.43$, $h_2 = -0.69$ and $h_3 = -1.1$. For different values of m the series solutions are calculated and represented in Table 2. It is notice from this table that the series (32) converges in the total area of λ. The graphs of the ratio

$$\beta_f = \left| \frac{f_m(h)}{f_{m-1}(h)} \right|, \quad \beta_\theta = \left| \frac{\theta_m(h)}{\theta_{m-1}(h)} \right|, \quad \beta_S = \left| \frac{S_m(h)}{S_{m-1}(h)} \right|, \tag{35}$$

versus the number of terms m is represented in Figure 2. These figures indicates that the the series (33) converges to the exact solution.

5. Results and discussion

The influence of thermal radiation Rd on the velocity $f(\lambda)$, temperature $\theta(\lambda)$ and nanoparticle volume fraction $S(\lambda)$ is shown graphically in Figure 3. by taking the remaining parameters as $B_r = 0.5$, $P_r = 1.0$, $A = 1$, $Re = 5$, $N_b = 0.5$ and $N_r = 1.0$ and analyze the values of Nusselt number and nanoparticle sherwood number in presence of magnetic parameter Ha, thermal radiation Rd, ion-

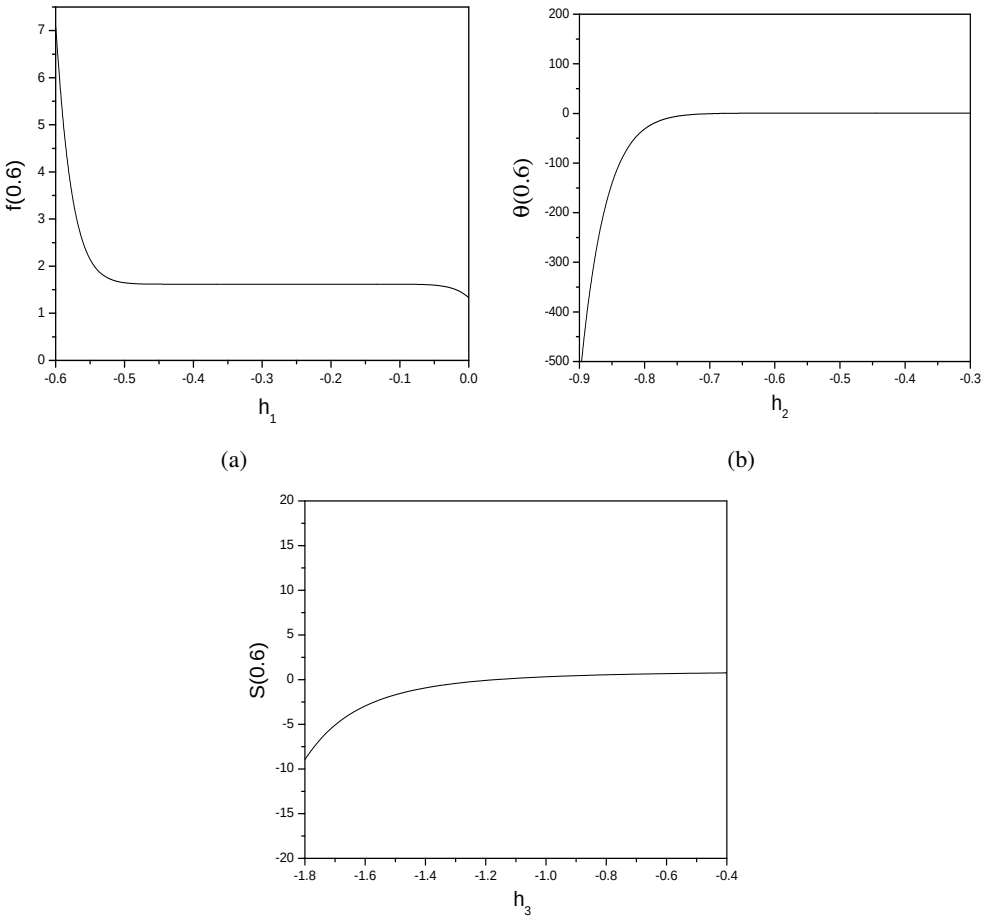

Figure 1. The h-curves of $f(\lambda), \theta(\lambda)$ and $S(\lambda)$ when $N_r = 1.0, N_t = 0.5, N_b = 0.5, Gr = 10.0, Ha = 5.0, A = 1.0, Re = 5.0, P_r = 1.0, Rd = 1.0, \beta_i = 2.0, \beta_h = 2.0, B_r = 0.5$.

slip parameter βi and Hall parameter β_h against the parameters N_t and Gr are shown graphically in Figures 4 - 7.

Figure 3 represents the impact of the thermal radiation Rd on dimensionless velocity in flow direction, temperature and nanoparticle volume fraction. Figure 3a reveals that there is a small decay in dimensionless velocity with an increase in Rd. Figure 3b illustrates that the dimensionless temperature $\theta(\lambda)$ decreases with enhance in Rd. Figure 3c represents that the nanoparticle concentration $S(\lambda)$ enhanced with an increment in Rd.

Figure 4 represents the impact of the magnetite parameter Ha on nanoparticle sherwood number and Nusselt number against thermophoresis parameters N_t. Figure 4a reveals that the Nusselt number Nu enhances with an growth in Ha. Figure 4b depicts that the nanoparticle sherwood number NSh rises as Ha increases.

The variation of nanoparticle sherwood number NSh and Nusselt number Nu against thermophoresis parameters N_t with Hall-parameter β_h is presented in Figure 5. It is noticed from Figure 5a that Nu decreases with a rise in the parameter β_h. There is a decay in a nanoparticle Sherwood

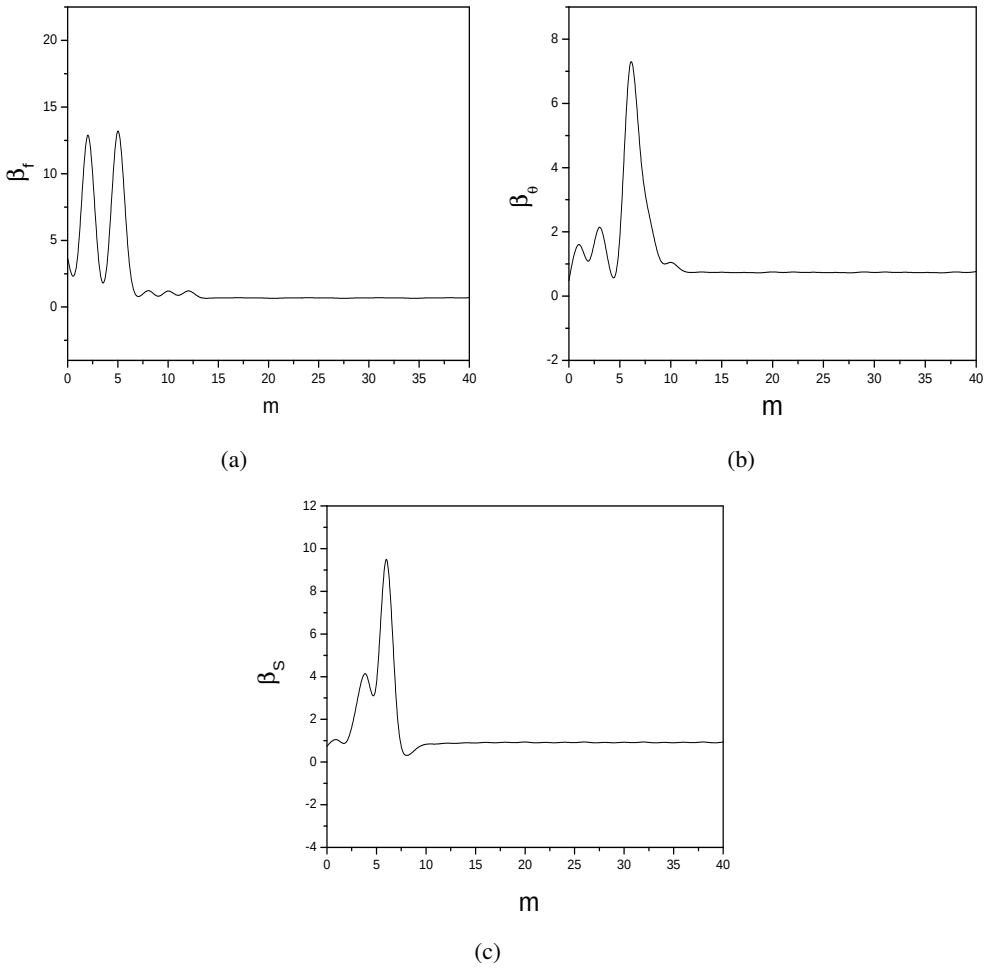

Figure 2. The ratios (a) β_f, (b) β_θ and (c) β_S from the theorem to reveal the convergence of the HAM solutions.

number NSh with a rise in β_h as depicted in Figure 5b. The inclusion of Hall parameter reduces the effective conductivity and hence drops the magnetite resistive force. Hence increase in β_h decreases the Nusselt number Nu and nanoparticle sherwood number NSh against thermophoresis parameters N_t.

The changes in Nusselt number Nu and nanoparticle sherwood number NSh against thermophoresis Nt with thermal radiation Rd is presented in Figure 6. It is noticed from Figure 6a that Nu decreases with a rise in Rd. There is an enhance in a nanoparticle sherwood number NSh with a rise in Rd as depicted in Figure 6b. Hence increase in Rd decreases Nu whereas increases nanoparticle sherwood number NSh against thermophoresis parameters N_t.

The impact of ion-slip parameter βi on Nusselt number and nanoparticle sherwood number against Grashof number Gr is depicted in Figure 7. It is observed from Figure 7a that, the Nusselt number decreases with a rise in the parameter βi. There is a decay in a nanoparticle Sherwood number NSh with a rise in βi as depicted in Figure 7b. The inclusion of ion-slip parameter reduces the effective conductivity and hence drops the magnetic resistive force. Hence increase in βi decreases Nu and NSh against Grashof number Gr.

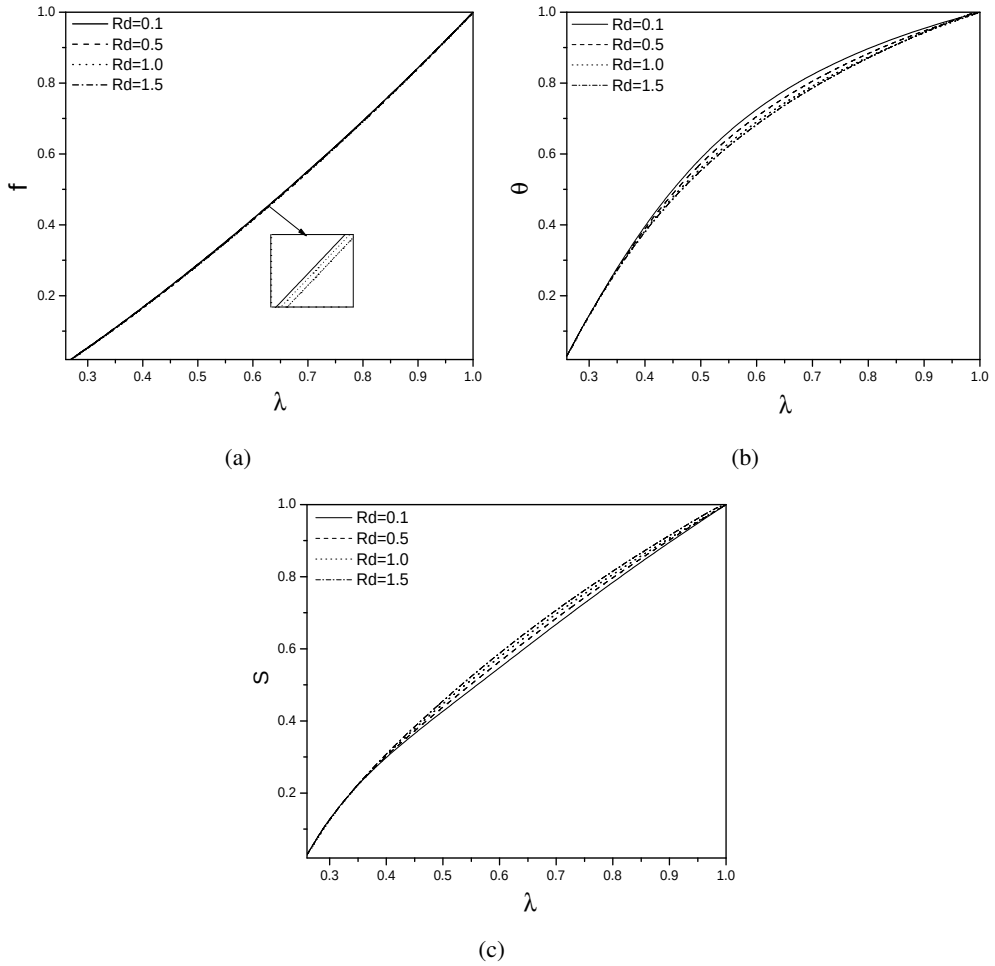

Figure 3. Effect of Radiation Rd on (a) Velocity, (b) Temperature and (c) Nanoparticle concentration profiles.

6. Conclusion

This article investigates the effects of thermal radiation, Hall and ion slip parameter on mixed convective flow of a nanofluid between two concentric coaxial cylinders considering magnetic field against the parameters N_t and Gr. The non-dimensional non-linear equations are solved by using Homotopy analysis method (HAM). The main findings are as follows

The dimensionless velocity, temperature decreases whereas nanoparticle concentration rises with an increase in thermal radiation parameter Rd. The Nusselt number Nu and nanoparticle Sherwood number NSh against thermophoresis parameters N_t raises with an increase in magnetic parameter. As an increase in the Hall parameter, the Nusselt number Nu, and nanoparticle Sherwood number NSh against thermophoresis parameters N_t are decreased. As an increase in thermal radiation Rd, the Nusselt number Nu decreases whereas nanoparticle Sherwood number NSh against thermophoresis parameters N_t are increases. As the ion slip parameter rises, the Nusselt number Nu and nanoparticle Sherwood number NSh against Grashof number Gr decreases.

REFERENCES

Ashorynejad, H.R., Abdulmajeed, A.M. and Mohsen, S. (2013). Magnetic field effects on natural convection flow of a nanofluid in a horizontal cylindrical annulus using Lattice Boltzmann method, International Journal of Thermal Science, Vol. 64, pp.240 - 250.

Buongiorno, J. (2006). Convective transport in nanofluids, ASME Journal of Heat Transfer, Vol.128, pp. 240 - 250.

Choi, S. U. S. (1995). *Enhancing thermal conductivity of fluids with nanoparticles*, In: Singer, D.A. and Wang, H.P., Eds., Development and Applications of Non-Newtonian Flows, American Society of Mechanical Engineers, New York, Vol. 66, pp.99-105.

Chamkha, A. J., Jena, S.K. and Mahapatra, S. K.(2015). MHD Convection of Nanofluids: A Review, Journal of Nanofluids, Vol. 4, pp. 271 - 292.

Das, S., Chakraborty, S., Jana, R.N., Makinde, O.D. (2015). Mixed convective Couette flow of reactive nanofluids between concentric vertical cylindrical pipes, J. Nanofluids. Vol. 4, pp. 485-493.

Dawood, H.K., Mohammed, H.A., Sidik, N.A.C., Munisamy, K.M. and Wahid, M.A. (2015). Forced, natural and mixed-convection heat transfer and fluid flow in annulus: A review, International Communications in Heat and Mass Transfer, Vol. 62, pp. 45 - 57.

Garg, B.P., Singh, K.D., Bansal, A.K. (2014). Hall current effect on viscoelastic (Walters liquid model-B) MHD oscillatory convective channel flow through a porous medium with heat radiation, Kragujevac Journal of Science, Vol. 36, pp.19-32.

Hazarika, G.C. (2014). Hall current in a rotating channel on MHD flow with radiation and viscous dissipation, International Journal of Scientific and Innovative Mathematical Research (IJSIMR) Volume 2, Issue 6, pp. 611-619.

Hayat, T., Shafique, M., Tanveer, A. and Alsaedi, A. (2016). Hall and ion slip effects on peristaltic flow of Jeffrey nanofluid with Joule heating, Journal of Magnetism and Magnetic Materials, Vol. 407(1), pp. 51 - 59.

Liao SJ. (2003). *Beyond perturbation. Introduction to homotopy analysis method*. Boca Raton:Chapman and Hall/CRC Press.

Liao SJ. (2004). On the homotopy analysis method for nonlinear problems. Applied Mathematics Computations, Vol. 147(2), pp. 499-513.

Liao SJ. (2010). An optimal homotopy-analysis approach for strongly nonlinear differential equations. Commun Nonlinear Sci Numer Simul, Vol.15, pp.200-316.

Liao, S.J. (2013). *Advances in the Homotopy Analysis Method.* World Scientific Publishing Company, Singapore.

Mozayyeni, H.R., Rahimi, A.B.(2012). Mixed convection in cylindrical annulus with rotating outer cylinder and constant magnetic field with an effect in the radial direction. Scientia Iranica, Vol. 19(1), pp.91-105.

Rajput, U.S. and Shareef, M. (2017). Unsteady MHD flow along exponentially accelerated vertical flat surface through porous medium with variable temperature and Hall current in a rotating system, J Fundam Appl Sci., Vol. 9(2), pp.1050-1062.

Rajput, U.S. and Gaurav Kumar (2018). Rotation and radiation effects on MHD flow past an inclined plate with variable wall temperature and mass diffusion in the presence of Hall current, Applications and Applied Mathematics (AAM) Volume 13, Issue 1, pp.484-495.

Ramana Reddy, J.V., Sugunamma, V., Sandeep, N. and Sulochana, C. (2016). Influence of chemical reaction, radiation and rotation on MHD nanofluid flow past a permeable flat plate in porous medium, Journal of the Nigerian Mathematical Society Vol. 35, pp. 48-65.

Ramesh Babu, K., Venkateswarlu, B. and Satyanarayana, P. V. (2014). Effects of chemical reaction and radiation absorption on mixed convective flow in a circular annulus at constant heat and mass flux, Advances in Applied Science Research, Vol. 5(5), pp. 122-138.

Satya Narayana, P.V., Venkateswarlu, B., Venkataramana, S.(2013). Effects of Hall current and radiation absorption on MHD micropolar fluid in a rotating system. Ain Shams Engineering J. Vol.4, pp.843-854.

Sheikholeslami, M. and Abelman, S. (2015).Two-phase simulation of nanofluid flow and heat transfer in an annulus in the presence of an axial magnetic field, IEEE Transactions on Nanotechnology, Vol. 14(3), pp. 561 - 569.

Sheikholeslami, M.,(2017). Influence of Lorentz forces on nanofluid flow in a porous cylinder considering Darcy model, Journal of Molecular Liquids, Vol. 225, pp. 903-912.

Sheikholeslami, M., (2017). Magnetic field influence on nanofluid thermal radiation in a cavity with tilted elliptic inner cylinder, Journal of Molecular Liquids, Volume 229, pp. 137- 147.

Srinivasacharya, D. and Shafeeurrahman, Md. (2017). Entropy Generation Due to MHD Mixed Convection of Nanofluid Between Two Concentric Cylinders with Radiation and Joule Heating Effects, Journal of Nanofluids, Vol. 6 (6), pp.1227-1237.

Srinivasacharya, D. and Shafeeurrahman, Md. (2017). Hall and ion slip effects on mixed convection flow of nanofluid between two concentric cylinders, Journal of the Association of Arab Universities for Basic and Applied Sciences, Vol. 23, pp.223-231.

Tani, I. (1962). Steady flow of conducting fluids in channels under transverse magnetic fields with consideration of Hall effects. Journal of Aerospace Science Vol. 29, pp. 297-305.

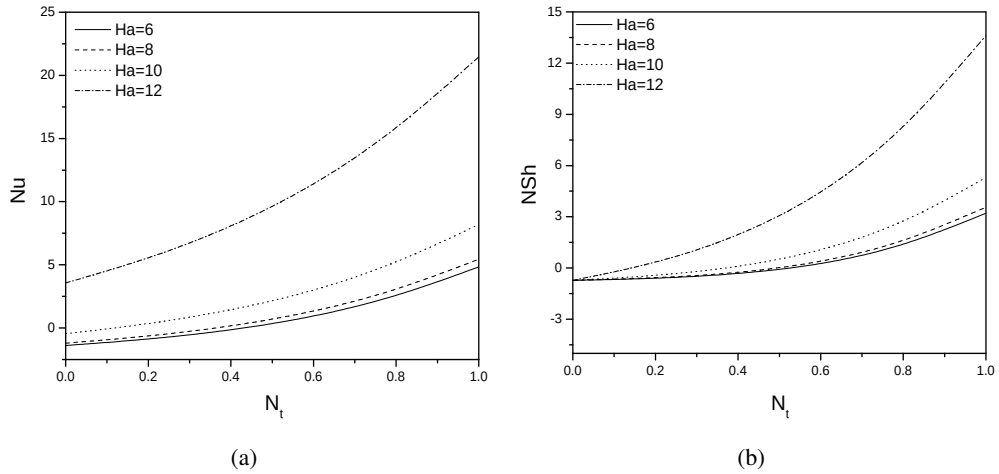

Figure 4. Effect of Ha on (a) Nusselt number (b) Nanoparticle Sherwood number versus thermophoresis parameters.

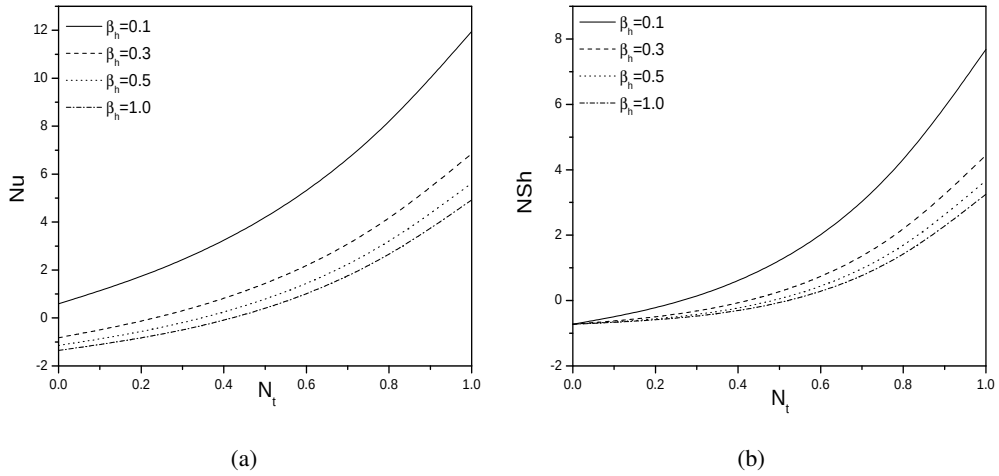

Figure 5. Effect of β_h on (a) Nusselt number,(b) Nanoparticle Sherwood number versus thermophoresis parameters.

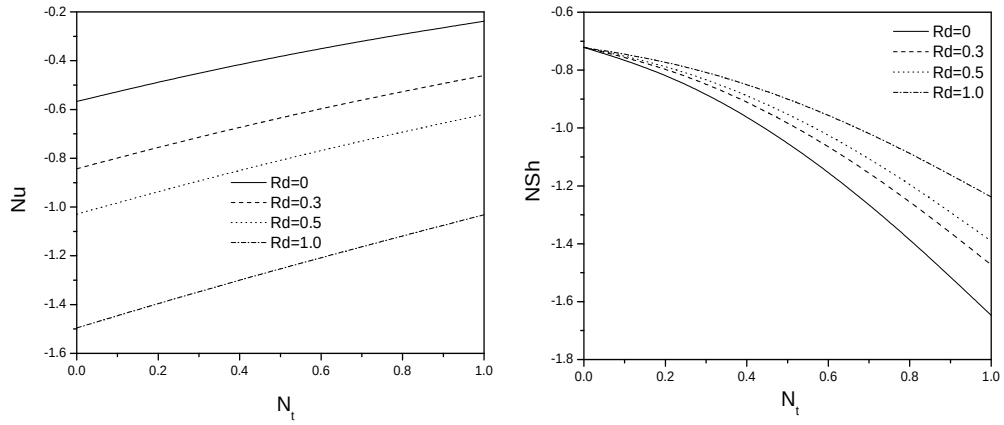

(a) (b)

Figure 6. Effect of Radiation Rd on (a) Nusselt number, (b) Nanoparticle Sherwood number versus thermophoresis parameters.

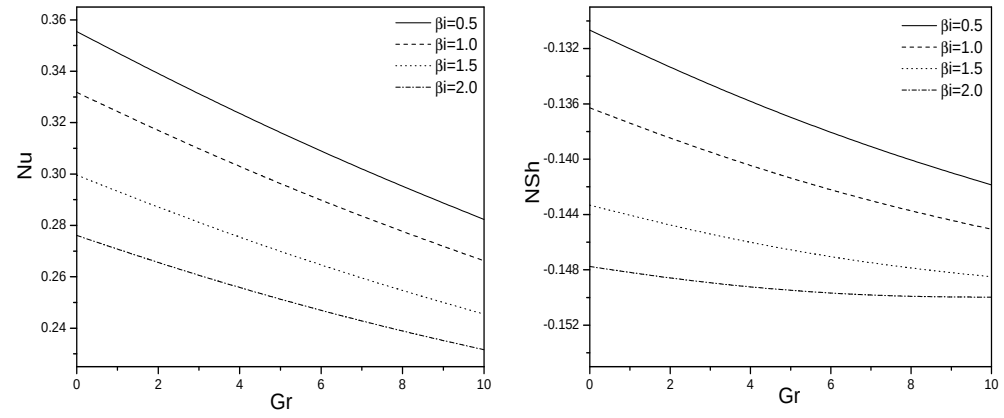

(a) (b)

Figure 7. Effect of βi on (a) Nusselt number, (b) Nanoparticle Sherwood number versus Grashof numbers.